Proc. Natl. Acad. Sci. USA
Vol. 91, pp. 11752–11756, November 1994
Cell Biology

Commitment to apoptosis is associated with changes in mitochondrial biogenesis and activity in cell lines conditionally immortalized with simian virus 40

(immortalization/mitochondria)

JEAN-LUC VAYSSIÈRE*, PATRICE X. PETIT, YANICK RISLER, AND BERNARD MIGNOTTE

Centre de Génétique Moléculaire, Centre National de la Recherche Scientifique, F-91198 Gif-sur-Yvette cedex, France

Communicated by Ruth Sager, July 20, 1994 (received for review March 11, 1994)

ABSTRACT **Rodent embryo cells immortalized with temperature-sensitive mutants of simian virus 40 large tumor (T) antigen have a proliferative potential that depends on temperature. At the restrictive temperature, heat-inactivation of large T antigen causes p53 release, growth arrest, and cell death. Morphological and molecular analysis indicate that the induced cell death corresponds to apoptosis. Flow cytometric analysis using a combination of forward light scatter and side scatter allows a discrimination of cells committed to apoptosis within the whole population. These cells display a reduction in cell size and a higher cellular density, confirming the apoptotic nature of the cell death. When cells exhibiting the morphological features of apoptosis were stained with a fluorescent probe of the mitochondrial membrane potential, a decreased accumulation of the dye was recorded. Measures of cellular respiration, performed with whole-cell populations, showed that the lower mitochondrial membrane potential ($\Delta\Psi_m$) correlates, as expected, with an uncoupling of electron transport from ATP production and is linked to the induction of apoptosis. We also show that this decrease in $\Delta\Psi_m$ is associated with a decrease in the rate of mitochondrial translation. These events are detected at early stages of the apoptotic process, when most of the cells are not irreversibly committed to death, suggesting that mitochondria could be a primary target during apoptosis.**

Mammalian cells grown in culture exhibit a finite life-span for proliferation. After a variable number of divisions they stop dividing, undergo a variety of changes, and finally die. Some oncogenes have the ability to confer an unlimited proliferative potential (immortality) to primary cells in culture. In the case of polyomavirus-induced immortalization of rodent embryo fibroblasts, it has been shown that the unlimited proliferative capacity is maintained by the large tumor (T) antigen (1–4). This implies that cells immortalized with temperature-sensitive mutants of large T antigen have a proliferative potential that depends on temperature. At the permissive temperature the cells are immortal, and upon shift to the restrictive temperature, heat-inactivation of large T antigen causes growth arrest and cell death. Two morphologically distinct types of cell death have been defined: necrosis and apoptosis. Necrosis is essentially accidental in its occurrence and results from severely injurious changes in the environment of the affected cells. In contrast, apoptosis is an active process of gene-directed cellular self-destruction and in most cases serves a biologically meaningful homeostatic function (5, 6). It has been observed that cell death induced in rat embryo cells that had been conditionally immortalized by simian virus 40 (SV40) large T antigen is associated with a release of p53 activity and exhibits morphological and biochemical features of apoptosis (7). With the aim of characterizing genetic and biochemical parameters involved in this process, we have undertaken the study of such conditionally immortal cell lines. The REtsAF cell line isolated from a rat embryo fibroblast culture (2) has been chosen as a model. We have previously shown that DNA replication is arrested less than 24 hr after the shift up to the restrictive temperature (39.5°C), whereas global transcription and translation rates are only slightly affected. However, a two-dimensional SDS/polyacrylamide electrophoresis analysis showed that nuclearly encoded mitochondrial proteins accumulate as their noncleaved cytoplasmic precursors at 39.5°C (8). We report here a flow cytometric study of the changes in cell morphology and mitochondrial membrane potential ($\Delta\Psi_m$) induced at 39.5°C in REtsAF. Cellular respiration and mitochondrial translation rates have also been monitored. Parallel experiments performed with the REtsAF-Rev1 variant and with a cell line (RELPB) immortalized by wild-type SV40 (2) allowed us to distinguish effects of the temperature shift from apoptosis-related changes.

MATERIALS AND METHODS

Cell Lines and Cell Culture. The REtsAF and RELPB cell lines were isolated at low cell density from a rat embryo fibroblast culture infected with SV40 (2). REtsAF was obtained by using a temperature-sensitive tsA58 mutant and is temperature sensitive for immortalization, whereas RELPB was obtained with wild-type SV40 and is immortal at both 33° and 39.5°C. REtsAF-Rev1 was derived from REtsAF by selection for proliferation at 39.5°C (8). Cells were propagated in Dulbecco's modified Eagle's medium (DMEM) supplemented with 10% (vol/vol) fetal calf serum, penicillin (100 μg/ml), and streptomycin (100 units/ml) under 5% CO_2/95% air. The cultures were screened regularly for the absence of mycoplasma.

Flow Cytometry. For mitochondrial membrane potential measurements, cells (about 10^6 per ml) were incubated in culture medium with 0.1 μM 3,3′-dihexyloxacarbocyanine [$DiOC_6(3)$] (Molecular Probes) for 30 min at 33°C. They were centrifuged to remove excess fluorochrome and resuspended in fresh culture medium before analysis. Control experiment was performed with 5 μM mClCCP (carbamoyl cyanide *m*-chlorophenylhydrazone), an uncoupling agent that abolishes the mitochondrial membrane potential (9). Plasma membrane integrity was monitored by measuring cell permeability to ethidium bromide (EtdBr) at 0.1 μg/ml (Molecular Probes). EtdBr molecules fluoresce intensely only when

The publication costs of this article were defrayed in part by page charge payment. This article must therefore be hereby marked "*advertisement*" in accordance with 18 U.S.C. §1734 solely to indicate this fact.

Abbreviations: T antigen, large tumor antigen; SV40, simian virus 40; $\Delta\Psi_m$, mitochondrial membrane potential; $DiOC_6(3)$, 3,3′-dihexyloxacarbocyanine; EtdBr, ethidium bromide; FSC, forward scatter; SSC, side-angle scatter; mClCCP, carbamoyl cyanide *m*-chlorophenylhydrazone; FCCP, carbonyl cyanide *p*-trifluoromethoxyphenylhydrazone.

*To whom reprint requests should be addressed.

bound to double-stranded nucleic acids and can only be incorporated into cells when plasma membranes lose their selective permeability. The incubation time was 5 min at room temperature.

Flow cytometry measurements were performed with an EPICS V flow cytometer (Coulter) equipped with an argon laser (Spectra-Physics 2025-05). A standard 76-μm nozzle was used. The sheath was water at 4°C. For the cyanine dye $DiOC_6(3)$ (10), emission filters were 515-nm long-pass interference and 515-nm short-pass interference for PMT1 (green fluorescence). For EtdBr the emission filter was 610 nm LP for PMT2 (red fluorescence). The excitation was 488 nm at 400 mW. The count rate was 1500–2000 objects per sec. The resultant histograms were taken on 10^5 particles analyzed, and each histogram is representative of two to five independent preparations. For further analysis and comparison of data, results were converted into linear fluorescence units by using the following formula: $[fluo_{lin}] = 10^{[(fluo_{log} \times d/c]}$ (where "c" is the number of channels and "d" is the number of decades of the cytometer scale).

Statically delimited "bit-maps" allowed us to ascribe forward scatter (FSC) or side-angle scatter (SSC) to individual subpopulations formed by 100% of "intact cells" or 100% of apoptotic cells devoid of debris or aggregates. The working "bit-maps" are described in Fig. 1 as map1 (normal cells) and map2 (apoptotic cells).

Oxygen Consumption. Oxygen consumption of whole cells was measured polarographically with a Clark-type microelectrode in a 2-ml cell. Cells were grown at 33°C and shifted to 39.5°C for various periods of times. They were then harvested, and O_2 uptake was measured in fresh culture medium (11). Measurements were performed at 33°C, since preliminary studies had shown that similar results are obtained at 33°C or 39.5°C (data not shown). Oligomycin (Sigma), an inhibitor of mitochondrial ATPase, was used at a concentration of 2 μg/ml, and carbonyl cyanide p-trifluoromethoxyphenylhydrazone (FCCP) (Sigma), an uncoupler of oxidative phosphorylation that abolishes the mitochondrial membrane potential, was used at 5 μM (12). The standard deviation of independent preparations was 10%.

Mitochondrial Protein Synthesis. Cells were cultured for 30 min in fresh medium lacking methionine (J. Boy, Reims, France) in the presence of emetine (100 μg/ml; Sigma), an inhibitor of cytoplasmic protein synthesis, and they were then labeled with [^{35}S]methionine (37 TBq/mmol) at a concentration of 1.67 MBq/ml and incubated for 2 hr prior to harvesting. Cells were washed and harvested, and mitochondria were purified as described (11). Samples of mitochondrial proteins were run on SDS/polyacrylamide gels containing 15% acrylamide and 0.2% methylenebisacrylamide. Gels were incubated for 30 min in Amplify (Amersham) before drying and autoradiography with Amersham Hyperfilm. Proteins encoded by mitochondrial DNA were identified as described (13).

RESULTS

Flow Cytometry Analysis of Cell Death. As a first step, we examined the morphological changes occurring upon shift up to 39.5°C by flow cytometry. A combination of light FSC and SSC allows an estimate of cell size and cell density, respectively (14). To distinguish effects of the temperature shift from apoptosis-related changes, we also studied two distinct temperature-insensitive cell lines: the REtsAF-Rev1 variant and a cell line (RELPB) established by infection with wild-type SV40 (2).

Fig. 1 shows flow cytometric analysis of REtsAF cells under permissive and restrictive conditions. Cells can easily be discriminated from debris by their ability to exclude EtdBr. They located in an area called map1 under the permissive condition, whereas debris located in the left part of Fig. 1*A*. After a shift to the restrictive condition, this initial population became two well-separated cell subpopulations. One was of high FSC and corresponded to the highest FSC cell subpopulation present in map1 of Fig. 1*A*; the other (map2) was characterized by a significant decrease in FSC (from channel 37 in map1 to channel 15 in map2) and a slight increase in SSC (36 to 38), reflecting a reduction of cell size and a higher cellular density (compare *A* and *B* in Fig. 1). This new cell population did not overlap with the population of cells grown under permissive conditions. Table 1 shows the evolution of the repartition of the cells between map1 and map2 in REtsAF and REtsAF-Rev1. In the temperature-insensitive variant (REtsAF-Rev1), less than 0.5% of the cells were found in map2 whatever the temperature (a similar result is obtained with RELPB, data not shown). Conversely,

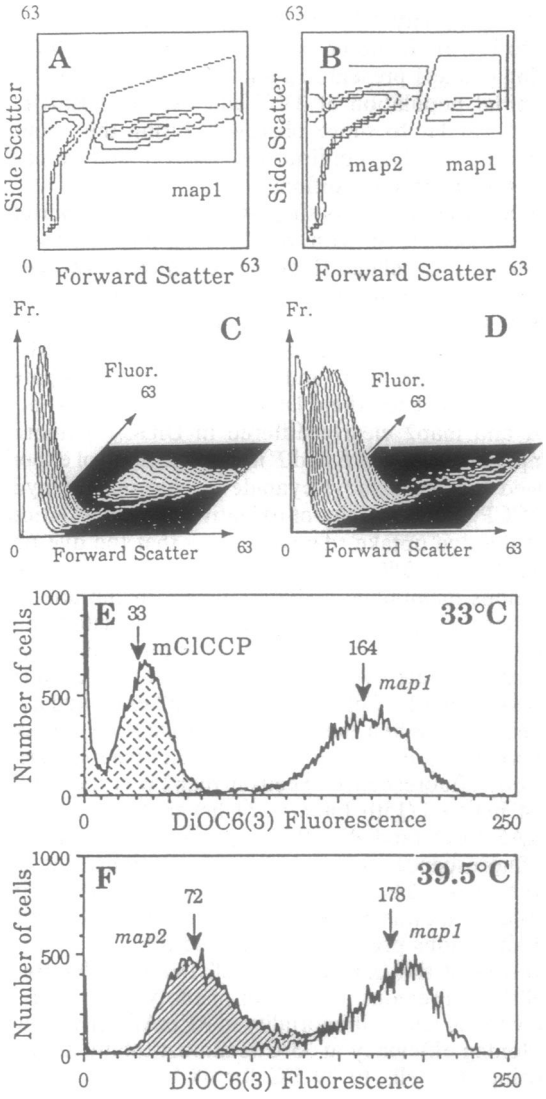

FIG. 1. Flow cytometric density maps and fluorescence histograms of REtsAF. Control cells maintained at 33°C and cells shifted for 24 hr at restrictive temperature (39.5°C) were studied for their light-scattering properties—i.e., SSC "cellular density" versus FSC "size" (*A* and *B*) or the membrane potential $DiOC_6(3)$ fluorescence versus FSC (*C* and *D*) (data taken on 64 channels). Two subpopulations may be designed as map1 and map2. The fluorescence histograms of cells considered in map1 and map2 are presented in *E* and *F* (the fluorescence values are given in arbitrary units on 256 channels). A control experiment with 5 μM mClCCP added as a decoupling agent prior to addition of the fluorescence dye is also shown (*E*).

Table 1. Flow cytometric analysis of cellular changes associated with cell death

Cell line	Time at 39.5°C, hr	Cells in map1			Cells in map2		
		%	Cells excluding EtdBr, %	Mean $DiOC_6(3)$ fluorescence	%	Cells excluding EtdBr, %	Mean $DiOC_6(3)$ fluorescence
REtsAF	0	>99.5	99	152	<0.5	–	–
	4	60	98	164	40	93	68
	8	44	98	164	56	78	66
	24	9	98	177	91	74	72
REtsAF-Rev1	0	>99.5	99	148	<0.5	–	–
	24	>99.5	99	156	<0.5	–	–

in REtsAF after the shift to 39.5°C, the proportion of cells found in map2 progressively increased and reached 91% after 24 hr. A study of EtdBr exclusion indicated that the plasma membrane integrity of cells shifted to map2 was unaffected during the early phase of this process. Furthermore, after 24 hr at 39.5°C, only 26% of these cells became slightly permeable to EtdBr. It should be noticed that the fraction of cells staying in map1 presented a higher mean FSC and SSC than the initial population at 33°C and excluded EtdBr. These results, similar to those observed during the apoptosis of other cells (15–17), confirm the apoptotic nature of the cell death under these conditions.

Since previous results suggested that mitochondrial failure may be associated with the loss of immortality (8), we examined $\Delta\Psi_m$-related fluorescence in these two cell populations by measuring their ability to accumulate $DiOC_6(3)$. After a shift to 39.5°C, a cell population exhibiting both a lower $DiOC_6(3)$ uptake and a lower FSC was clearly visible (compare cytograms *C* and *D* in Fig. 1). When gated cells were examined for their $DiOC_6(3)$ uptake, cells located in map1 and map2 clearly differed in $DiOC_6(3)$ fluorescence (compare histograms *E* and *F* in Fig. 1). Control experiments showed that carbamoyl cyanide *m*-chlorophenylhydrazone (mClCCP), an uncoupler of oxidative phosphorylation, abolished the dye uptake, demonstrating that the dye uptake is driven by the $\Delta\Psi_m$ (Fig. 1*E*). The cells under restrictive conditions maintained a slightly higher membrane potential than those treated with mClCCP (compare histograms *E* and *F* in Fig. 1), which shows that they are not fully uncoupled. We analyzed the evolution of $DiOC_6(3)$ uptake during this process (Table 1). Cells located in map2 exhibited a reduced fluorescence. When the measures of $DiOC_6(3)$ uptake were converted into linear fluorescence units (see *Materials and Methods*), fluorescence of cells in map2 was about 1/12th (at t = 4 hr) to 1/15th (at t = 24 hr) that of cells in map1. REtsAF-Rev1 (and RELPB, data not shown) maintained a high fluorescence under restrictive conditions. These results show that the $\Delta\Psi_m$ of REtsAF cells decreases during apoptosis and that this process could be related to the mitochondrial alterations previously described (8).

Kinetics of the Induction of Cell Death Under Restrictive Conditions. Previous analysis of phenotypic changes associated with the loss of immortality in REtsAF cells showed that the cloning efficiency at 33°C is almost totally abolished by exposing the cells to 39.5°C for 48 hr (2). To establish a chronology of the events, we determined the time at which the cells are irreversibly committed to death. For this purpose, we measured the fraction of cells able to resume growth under permissive conditions (33°C) after various periods of incubation under restrictive conditions (39.5°C). Fig. 2 shows that, after about 15 hr at 39.5°C, 50% of the cells irreversibly lost their proliferative capacity. The figure also shows that DNA fragmentation and alterations in the plasma membrane, which are commonly used as markers of apoptosis, occurred a long time after this irreversible event. Thus, the morphological changes, which occur simultaneously with the drop of $\Delta\Psi_m$, are early events during the process.

Cellular Respiration Under Permissive and Restrictive Conditions. The decrease in $DiOC_6(3)$ uptake suggests that respiratory activity may be impaired when REtsAF cells are induced to apoptose. We measured the rate of oxygen consumption in REtsAF, REtsAF-Rev1, and RELPB whole cells (basal respiration). Addition of oligomycin allowed us to estimate oxidative phosphorylation coupled to respiration, and the use of an uncoupler (FCCP) indicated the maximal respiratory rate (oxidative capacity). We then defined the respiratory control as the ratio of these two values with the aim of quantifying the coupling state and thus the functional state of the mitochondria. When shifted to 39.5°C, basal oxygen consumption by REtsAF cells increased (Table 2). However, the sensitivity of oxygen consumption to oligomycin decreased and respiratory control diminished, reflecting an uncoupling of electron transport from ATP production. Therefore, the observed reduction in $DiOC_6(3)$ fluorescence could be attributed to a lower mitochondrial $\Delta\Psi_m$. In the two control cell lines (REtsAF-Rev1 and RELPB), the observed increase of basal respiration and of respiratory control reflects an augmentation of the oxidative capacity and a stimulation of the mitochondrial energetics associated with the shift up to 39.5°C (Table 2 and data not shown).

These results show that temperature shift to 39.5°C leads to an increase in mitochondrial activity in nonconditional cell lines but to an uncoupling of oxidative phosphorylation in sensitive cells. This uncoupling could be related to the collapse of the mitochondrial membrane potential observed by flow cytometry.

Mitochondrial Protein Synthesis. The mitochondrial dysfunctions described above led us to study mitochondrial biogenesis during the shift to restrictive temperature. We

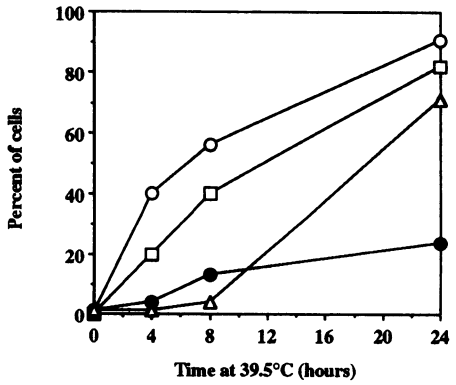

FIG. 2. Kinetics of the loss of cell viability. One thousand REtsAF cells were plated at 33°C for 15 hr, shifted to 39.5°C for the indicated time, and then shifted back to 33°C. After 12 days at 33°C, the number of clones was counted. Alternatively, subconfluent cultures of REtsAF were shifted up to 39.5°C for various times, and then the cloning efficiency was measured. Both experiments gave the same kinetics (□). The percentage of cells locating in map2 (○) and of cells not excluding EtdBr (●) are plotted. The percentage of cells that exhibit DNA fragmentation (7), as measured by flow cytometry, is also shown (△).

Table 2. Oxygen consumption in REtsAF and REtsAF-Rev1

Cell line	Time at 39.5°C, hr	Oxygen consumption, nmol of O/min per mg of protein: Basal	With oligomycin	With FCCP	Respiratory control
REtsAF	0	23.5	13.2	30.6	2.2
	4	30.3	16.5	36.4	2.2
	8	28.1	18.3	28.1	1.5
	24	51.3	36.7	51.3	1.3
	48	51.6	44.0	46.4	1.1
REtsAF-Rev1	0	14.6	7.3	21.0	2.9
	48	18.7	7.3	37.4	5.1

Cells were grown at 33°C and shifted to 39.5°C for the indicated times. They were then harvested and O_2 uptake measured.

analyzed the accumulation of new mitochondrial protein in the three cell lines upon shift to 39.5°C. Fig. 3 shows that at 39.5°C, mitochondrial synthesis in REtsAF rapidly decreased after a transient increase observed at 5 hr. In contrast, mitochondrial protein synthesis in the two nonconditional lines REtsAF-Rev1 and RELPB was stably increased at 39.5°C. This observation shows that the induction of apoptosis in REtsAF cells is accompanied by alterations in both mitochondrial biogenesis and function. These alterations in mitochondrial protein synthesis are not associated with mitochondrial DNA fragmentation (data not shown), which suggests that, as described for thymocytes and mastocytoma cells (18), DNA degradation during apoptosis is a specific nuclear event. Furthermore, the levels of mitochondrial DNA and mitochondrial RNA remain approximately constant, suggesting that the mitochondrial biogenesis dysfunction at 39.5°C results from a postranscriptional disturbance.

DISCUSSION

The experiments described above demonstrate a correlation between the induction of the apoptotic process and defects in mitochondrial biogenesis and function. Flow cytometry studies allowed us to detect the appearance of a subpopulation of cells harboring distinct morphologic properties corresponding to apoptose-induced cells. These cells also display a lower mitochondrial membrane potential [measured by $DiOC_6(3)$ uptake]. After a 4-hr shift to the restrictive condition (i.e., at an early stage of the apoptotic process), these changes are detected in about 40% of the adherent cells, whereas no fragmentation of nuclear DNA can be detected (7) and, until 8 hr at restrictive temperature, a large fraction of cells in this subpopulation are not irreversibly induced to die. It should also be noted that cellular membranes and the mitochondrial DNA are not damaged during the process. Thus, these changes are not the consequence of a generalized damage to cellular structures. The defects in mitochondrial respiration and translation are detected only after 8 hr at 39.5°C. However, these observations, obtained with the whole population of attached cells, add changes affecting apoptotic and nonapoptotic cells. We can hypothesize that stimulation of mitochondrial biogenesis and respiration, observed transiently during the first 4 of 5 hr in REtsAF and stably in control nonconditional cell lines, reflects changes associated with the shift at 39.5°C. Since mitochondrial translation has been reported to be dependent on $\Delta\Psi_m$ (19–21), the decrease in $\Delta\Psi_m$ could be responsible for the drop of mitochondrial translation. This decrease could also account for the uncoupling of oxidative phosphorylation (22) and the defects in maturation of cytoplasmic precursors (23) previously observed (8).

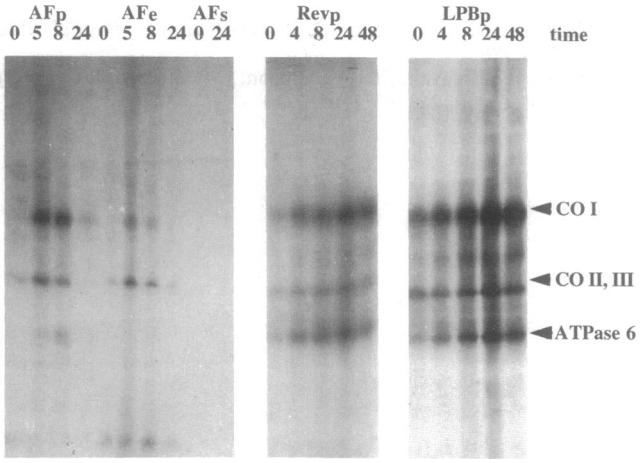

FIG. 3. Mitochondrial protein synthesis in REtsAF, REtsAF-Rev1, and RELPB. Shown are fluorograms, after electrophoresis through a SDS/polyacrylamide gel, of the mitochondrial translation products labeled with [^{35}S]methionine at various times after the shift to 39.5°C. The cultures were labeled in the presence of emetine (100 μg/ml) for 2 hr. Mitochondria were purified, and samples (50 μg) were run on SDS/polyacrylamide gel. Controls with crude extracts and postmitochondrial supernatants were also shown for REtsAF. CO I, CO II, and CO III, subunits I, II, and III of cytochrome oxidase; ATP6, subunit 6 of the ATP synthetase; AF, REtsAF; Rev, REtsAF-Rev1; LPB, RELPB; and subscripts p, e, and s, mitochondrial pellet, crude extract, and postmitochondrial supernatant, respectively.

The drop of mitochondrial membrane potential, associated with the induction of apoptosis in REtsAF cells at 39.5°C, can be observed if apoptosis is induced in REtsAF by another means (high cellular density). Furthermore, a similar observation has been made during dexamethasone-induced thymocyte apoptosis (P.X.P., H. Lecoeur, E. Zorn, C. Dauguet, B.M., and M. L. Gougeon, unpublished results). Thus, the mitochondrial changes reported here are not a peculiarity of the cellular model described here.

Defects in some mitochondrial functions have been associated previously with apoptosis (24–26). However, to our knowledge, such study of mitochondrial function and biogenesis during apoptosis has never been performed. In the case of tumor necrosis factor α (TNFα) cytotoxicity (27), early disruption of mitochondrial function (28, 29) has been described. Furthermore, depletion of the mitochondrial electron transport abrogates the cytotoxic effect of TNFα (30). In the same system, the overexpression of *Bcl2* has been shown to increase $\Delta\Psi_m$, and this effect could be linked to its antiapoptotic activity because the ionophore nigericin, known to increase $\Delta\Psi_m$, has a similar effect (31).

The finding that the *Bcl2* protooncogene product can locate to mitochondrial membrane (32) and that its ability to suppress apoptosis is reduced in constructs that lack the C-terminal transmembrane segment (33, 34) has suggested that mitochondrial function could be impaired during apoptosis and that Bcl2 could counteract this event. Since it has been found that Bcl2 blocks apoptosis in cells that do not contain a functional respiratory chain (cells lacking mtDNA) (35), it has been concluded that the Bcl2 activity is not related to mitochondrial respiration. However, it should be noted that these cells, selected for their ability to grow in the absence of respiration, maintain a normal $\Delta\Psi_m$ (ref. 36 and our unpublished results).

The origin of the drop in mitochondrial membrane potential remains to be determined. Taking into account that (*i*) Bcl2 functions in an antioxidant pathway to prevent apoptosis (34, 37), (*ii*) prooxidants induce calcium release from mitochondria (38), and (*iii*) $\Delta\Psi_m$ is dependent on calcium uptake (39), it is tempting to speculate that calcium redistribution could mediate the decrease of $\Delta\Psi_m$. Indeed, a repartitioning of

intracellular calcium has been observed during apoptosis of an interleukin 3-dependent hematopoietic cell line (40).

We thank Dr. J. Feunteun for helpful discussions; Drs. R. Sager, J. C. Mounolou, and W. Hauswirth and M. G. Wallis for their critical reading of the manuscript; and N. Glab for her kind hospitality to conduct oxigraphic measurements. This work was supported in part by a grant from the Association pour la Recherche Contre le Cancer (no. 6960) and by the Université de Versailles/Saint-Quentin.

1. Rassoulzadegan, M., Naghashfar, Z., Cowie, A., Carr, A., Grisoni, M., Kamen, R. & Cuzin, F. (1983) *Proc. Natl. Acad. Sci. USA* **80**, 4354–4358.
2. Petit, C. A., Gardes, M. Y. & Feunteun, J. (1983) *Virology* **127**, 74–82.
3. Jat, P. S. & Sharp, P. A. (1989) *Mol. Cell. Biol.* **9**, 1672–1681.
4. Jacquemin-Sablon, H., Ganz, L. & Feunteun, J. (1990) *Biol. Cell* **68**, 227–230.
5. Bursch, W., Oberhammer, F. & Schulte-Hermann, R. (1992) *Trends Pharmacol. Sci.* **13**, 245–251.
6. Tomei, L. D. & Cope, F. O. (1991) *Apoptosis: The Molecular Basis of Cell Death*, eds. Inglis, J. & Witkowski, J. A. (Cold Spring Harbor Lab. Press, Plainview, NY).
7. Zheng, D. Q., Vayssière, J. L., Lecoeur, H., Petit, P. X., Spatz, A., Mignotte, B. & Feunteun, J. (1994) *Oncogene* **9**, 3345–3351.
8. Mignotte, B., Larcher, J. C., Zheng, D. Q., Esnault, C., Coulaud, D. & Feunteun, J. (1990) *Oncogene* **5**, 1529–1533.
9. Glab, N., Petit, P. X. & Slonimski, P. P. (1993) *Mol. Gen. Genet.* **236**, 299–308.
10. Korchak, H. M., Rich, A. M. & Wilkenfeld, C. (1982) *Biochem. Biophys. Res. Commun.* **108**, 1495–1501.
11. Vayssière, J. L., Larcher, J. C., Berthelot, F., Benlot, C., Gros, F. & Croizat, B. (1986) *Biochem. Biophys. Res. Commun.* **140**, 789–796.
12. Vayssière, J. L., Cordeau-Lossouarn, L., Larcher, J. C., Basseville, M., Gros, F. & Croizat, B. (1992) *In Vitro Cell. Dev. Biol.* **28A**, 763–772.
13. Cordeau-Lossouarn, L., Vayssière, J. L., Larcher, J. C., Gros, F. & Croizat, B. (1991) *Biol. Cell* **71**, 57–65.
14. Darzynkiewicz, Z., Bruno, S., Delbino, G., Gorczyca, W., Hotz, M. A., Lassota, P. & Traganos, F. (1992) *Cytometry* **13**, 795–808.
15. Nicoletti, I., Migliorati, G., Pagliacci, M. C., Grignani, F. & Riccardi, C. (1991) *J. Immunol. Methods* **139**, 271–279.
16. Swat, W., Ignatowicz, L. & Kisielow, P. (1991) *J. Immunol. Methods* **137**, 79–87.
17. Shi, Y., Glynn, J. M., Guilbert, L. J., Cotter, T. G., Bissonnette, R. D. & Green, D. R. (1992) *Science* **257**, 212–214.
18. Murgia, M., Pizzo, P., Sandona, D., Zanovello, P., Rizzuto, R. & DiVirgilo, F. (1992) *J. Biol. Chem.* **267**, 10939–10941.
19. Coté, C., Boulet, D. & Poirier, J. (1990) *J. Biol. Chem.* **265**, 7532–7538.
20. Attardi, G. & Schatz, G. (1988) *Annu. Rev. Cell Biol.* **4**, 289–333.
21. Rabinovitz, Y. M., Pinus, H. A. & Kotelnikovo, A. V. (1977) *Mol. Cell. Biochem.* **14**, 109–113.
22. Hatefi, Y. (1985) *Annu. Rev. Biochem.* **54**, 1015–1029.
23. Glick, B. & Schatz, G. (1991) *Annu. Rev. Genet.* **25**, 21–44.
24. Nordeen, S. K. & Young, D. A. (1976) *J. Biol. Chem.* **251**, 7295–7303.
25. Vukmanovic, S. & Zamoyska, R. (1991) *Eur. J. Immunol.* **21**, 419–424.
26. Zoeteweij, J. P., Van De Water, B., De Bont, H. J. G. M., Mulder, G. J. & Nagelkerke, J. F. (1992) *Biochem. J.* **288**, 207–213.
27. Laster, S. M., Wood, J. G. & Gooding, L. (1988) *J. Immunol.* **141**, 2629–2634.
28. Lancaster, J. R., Laster, S. M. & Gooding, L. R. (1989) *FEBS Lett.* **248**, 169–174.
29. Schulze-Osthoff, K., Bakker, A. C., Vanhaesebroeck, B., Beyaert, R., Jacob, W. A. & Fiers, W. (1992) *J. Biol. Chem.* **267**, 5317–5323.
30. Schulze-Osthoff, K., Beyaert, R., Vandevoorde, V., Haegeman, G. & Fiers, W. (1993) *EMBO J.* **12**, 3095–3104.
31. Hennet, T., Bertoni, G., Richter, C. & Peterhans, E. (1993) *Cancer Res.* **53**, 1456–1460.
32. Hockenbery, D., Nunez, G., Milliman, C., Schreiber, R. D. & Korsmeyer, S. J. (1990) *Nature (London)* **348**, 334–336.
33. Alnemri, E. S., Robertson, N. M., Fernandes, T. F., Croce, C. M. & Litwack, G. (1992) *Proc. Natl. Acad. Sci. USA* **89**, 7295–7299.
34. Hockenbery, D. M., Oltvai, Z. N., Yin, X. M., Milliman, C. L. & Korsmeyer, S. J. (1993) *Cell* **75**, 241–251.
35. Jacobson, M. D., Burne, J. F., King, M. P., Miyashita, T., Reed, J. C. & Raff, M. C. (1993) *Nature (London)* **361**, 365–369.
36. Skowronek, P., Haferkamp, O. & Rodel, G. (1992) *Biochem. Biophys. Res. Commun.* **187**, 991–998.
37. Kane, D. J., Sarafian, T. A., Anton, R., Hahn, H., Gralla, E. B., Valentine, J. S., Ord, T. & Bredesen, D. E. (1993) *Science* **262**, 1274–1277.
38. Richter, C. & Kass, G. E. N. (1991) *Chem. Biol. Interact.* **77**, 1–23.
39. Gunter, T. E. & Pfeiffer, D. R. (1990) *Am. J. Physiol.* **258**, C755–C786.
40. Baffy, G., Miyashita, T., Williamson, J. R. & Reed, J. C. (1993) *J. Biol. Chem.* **268**, 6511–6519.